Carbonatites in oceanic hot spots

Max W. Schmidt[1] and Daniel Weidendorfer[2]

[1]ETH, Zurich, Switzerland, max.schmidt@erdw.ethz.ch
[2]Caltech, Pasadena, USA, danielwe@gps.caltech.edu

SUPPLEMENTARY MATERIAL

METHODS

Data were compiled from the pre-sorted georoc database ocean island files (http://georoc.mpch-mainz.gwdg.de/georoc/). Hot spots such as Aetna or Samoa with geotectonically complex situations and possible direct interference with subduction were avoided; otherwise we used those with sufficiently large data sets. Each file was filtered for analyses with 95-101.5 wt% totals, samples outside this range or listed as altered were excluded. All bulk rock compositions are then normalized to 100 wt% total on a volatile free basis with all Fe as FeO.
The histogram of total alkalis for extrusives shows a clear cut-off to <1.4 wt% K_2O+Na_2O. Of e.g. 9'000 extrusives of the Hawaiian hotspot only 24 are below this values, these are essentially from three publications (without geographical coherence), suggesting that these rocks were altered or possibly have an analytical problem; this is corroborated by a K_2O/Na_2O ranging from 0.01 to 2 for these 24 samples. We have hence excluded all rocks with <1.4 wt% Na_2O+K_2O.
Similarly, we did not accept trace element concentrations measured by XRF that are below 5-15 ppm (depending on the element).

Within each ocean island, rocks were sorted for

(i) Those with X_{Mg}>0.77 and/or Ni>650 ppm, this group is mostly olivine cumulative and was excluded from all plots.
(ii) Primitive melts were designated when X_{Mg}=0.77-0.65, which corresponds to equilibrium with olivine of Fo_{92-88} at 5-15 mol% Fe^{3+} (of Fe^{tot}), and Ni=150-650 ppm, corresponding to roughly 2000-4500 ppm Ni in mantle olivine (note that the $K_D^{olivine/melt}$ of Ni strongly depends on temperature, hence this range is chosen rather large).
(iii) To enlarge the dataset, rocks with 0.55<X_{Mg}<0.65 were plotted together with the primitive melts in Figs. 3 and A4, in this X_{Mg}-range olivine is the dominant fractionating mineral, minor fractionating cpx will not strongly modify trace element contents.
(iv) Intrusives were separated from subvolcanics, extrusives and dikes, intrusives are not plotted on the figures.

Only ocean islands with >100 analyses were retained, the dataset sorted for the above criteria contains 124-198 analyses for Pitcairn, Ascension, St. Helena and Tristan da Cunha; 242-331 for

the Comoro, Madeira and Society hotspots, 420 for Austral-Cook, 488 for the Kerguelen, 623 for the Marquesas, 824 for Galapagos, 885 for the Azores, 1'098 for Reunion-Mascarene, 1'152 for the Cape Verdes, 2'805 for the Canaries and 8'966 for the Hawaiian hotspot.

PRIMITIVE MELTS

Fig. 1 shows all volcanics, Fig. 1A is a subset of this figure with melts that are primitive, i.e. have $0.77>X_{Mg}>0.65$ and Ni=150-650 (the latter when measured). Primitive melts with <41 wt% SiO_2 are almost exclusively found on the Cape Verdes and Canaries but also for a few samples from the rejuvenated stages of Oahu Koolau and Kauai (Hawaiian hotspot see below).

CARBONATITES ON THE CAPE VERDES AND CANARIES, MELT INCLUSIONS

Cape Verdes: Carbonatites occur on 5 islands as dikes, stocks or large masses (Brava, Fogo, Mayo, Santiago, Santo Antao; Assunção et al. 1965; Machado et al. 1968; Hoernle et al. 2002; Holm et al. 2006; Madeira et al. 2010, Mourao et al. 2010).

Canaries: Carbonatite dikelets are reported only from Fuerteventura (Barrera et al. 1981, Balogh et al. 1999; Hoernle et al. 2002).

Melt inclusions: Averages are from Guzmics et al. (2011, 2012) for Keramasi (East African Rift); from Kogarko et al. (1991) and Panina (2005) for the Sibirian Guli intrusive and Krestovskiy massiv, respectively, which are about 50 km distant; and from Nielsen et al. (1997) for the Gardiner complex (East Greenland).

CARBONATITES ON HAWAII?

Primitive melts from the Hawaiian hot spot have mostly 45-52 wt% SiO_2 and 1.5-3.0 wt% Na_2O+K_2O (Fig. A1). The ~9'000 analyses are dominated by subalkaline to tholeiitic basalts and corresponding differentiation trends (Fig. A2a). SiO_2-undersaturated lavas are limited to the rejuvenates stages and Hilina bench, which were suspected to have a carbonatite association (Sisson et al., 2009): Low SiO_2 - high $(Na,K)_2O$ volcanics occur on Oahu (Waianae and Honolulu volcanic series; e.g. Macdonald and Katsura, 1964; Clague and Frey, 1982), in the rejuvenated volcanic stage of Maui (Kauai and Haleakala lavas; e.g. Macdonald and Katsura, 1964; Macdonald and Powers, 1968) and on East Molokai (e.g. Naughton et al., 1980). Sisson et al. (2009) reported basanite-nephelinite glass compositions from the submarine Hilina bench (Kilauea) that form a negative slope fractionation trend in the TAS diagram (Fig. A2a). In the Na_2O+K_2O – $SiO_2+TiO_2+Al_2O_3$ – $CaO+FeO+MgO$ ternary (Hamilton et al. 1979), only the most evolved Hilina bench samples reach the miscibility gap. However, whether carbonatites formed at Hilina bench

will probably remain elusive, as a preservation of carbonatites from submarine eruptions appears highly unlikely.

Further basanitic compositions with 2-5 wt% total alkalis are present at the Loihi Seamount (Frey and Clague, 1983) as well as within the volcanic centers of Mauna Kea and Kohala (Island of Hawaii; e.g. Macdonald and Katsura, 1964), these are more SiO_2-undersaturated and alkali-rich than the vast majority of Hawaiian lavas but not exceptional in terms of the global array.

Only the rejuvenated units of Kauai and Oahu Koolau have primitive samples with 38-42 wt% SiO_2, much lower than the other primitive melts from Hawaii. These units could potentially yield carbonatites through differentiation combined with immiscibility, nevertheless, melilite crystallization in these units (possibly a consequence of relatively high Al-contents) delimits alkali-contents in these fractionation series, preventing these magmas to reach alkali-contents near the melt miscibility gap. It remains to be seen whether one day carbonatites will be found on Hawaii, based on this analyses the above units are most prone.

TOTAL ALKALIS - SILICA DIAGRAM (TAS):

Note that the fractionation lines depicted here were originally used to define the sub-alkaline vs alkaline trends (Irvine and Baragar, 1971).

Carbonatite – silicate melt immiscibility: The "maximum extend of the miscibility gap" signifies that immiscibility does not occur at lower alkali contents than this limit, but that immiscibility must not necessarily set in once reaching this limit, e.g. CO_2-undersaturated or heavily peralkaline systems require higher alkali-contents for a given SiO_2. This limit is valid as long as carbonate is the dominant anionic species, P_2O_5- or F-rich carbonatites may differ.

Experiments that constrain the maximum extend of the miscibility gap are from Freestone and Hamilton (1980), Kjarsgaard (1998), Brooker and Kjarsgaard (2011), and Martin et al. (2013). Note that in earlier experiments rounded calcite had been interpreted as melt, however, this has been corrected by the original authors. Alkali-poor carbonatite quench interstitial to silicate minerals has also been reported as immiscible melt compositions, but experiments on the reported conjugated melt pairs have shown that the carbonatites were not immiscible melts, hence the alkali-poor carbonatite quench analyses did not represent melt compositions (Kjarsgaard, 1998; Martin et al., 2013).

Upper limit of fractionation: The system $NaAlSiO_3$-$KAlSiO_3$-SiO_2 constitutes the basis for highly evolved silicate melts. The Si-undersaturated alkali-feldspar – feldspathoid part of this system is well determined at 1 atm (volatile free, Schairer 1957) and 1, 2 and 5 kbar H_2O-pressure (Fudali 1963; Taylor and MacKenzie, 1975; Zeng and MacKenzie, 1984). For this study, the most important features of this phase diagram are the granite- (Tuttle and Bowen 1958, Luth et al. 1964) and phonolite-minima and the alkali-feldspar thermal divide in between. Of further interest are the cotectic lines extending from the phonolite minimum and leading on the K-rich side to invariant points that involve leucite and/or kalsilite (1 and 2 kbar) or to the K-spar – nepheline thermal maximum (at 5 kbar).

In this system, two major developments occur with pressure: (1) At low pressures, the solvus of the alkalifeldspars is below the liquidus surface and hence, on the alkali-feldspar join, there is only a minimum, which constitutes a thermal divide or maximum on the valley (in the liquidus surface) that connects the granite and phonolite minima. Nevertheless, any parent melt that reaches this valley cannot leave this line (under equilibrium crystallization) and will end up in one of the minima. Between 2 and 3 kbar, the alkali-feldspar solvus begins to intersect the liquidus surface, such that the granite and phonolite minima become eutectics and the connecting line in between a proper cotectic line. (2) With increasing pressure, the leucite liquidus field shrinks considerable such that the kalsilite and K-spar fields touch and the nature of the peritectics changes. As also the kalsilite field shrinks with pressure, such that the nepheline-K-spar cotectic develops a thermal divide or maximum at 5 kbar.
For the purpose of evolved OI melts, we plot the granite-minimum, the alkali-feldspar thermal divide (on the cotectic or the topological valley connecting the two minima), the phonolite minimum and the nepheline-alkalifeldspar cotectics into the TAS diagram.

Correction for other oxide components: The above minima, eutectica, and cotectics are plotted into the TAS diagram (thin grey line in Fig. 1a), but these compositions are strictly valid only for exactly meta-aluminous compositions in the haplo-system. Note that in such a system, Al_2O_3 is a dependent variable and cannot cause variations in total alkali vs. SiO_2. We have averaged CaO+FeO+MgO and peralkalinity of the 620 melts from the 17 oceanic hotspots that plot within 4 wt% SiO_2 of the thin grey line in Fig. 1a (i.e. the cotectics of the haplosystem) and obtain on average 4 wt% CaO+FeO+MgO and a peralkalinity of 1.1 ((K+Na)/Al), both values do not vary systematically along the above cotectics. Taking these average deviations from the strictly meta-aluminous haplo-system into account, the locations of the above cotectic lines, the alkali-feldspar thermal divide and the granite- and phonolite-minima/eutectics are replotted as thick grey line and fields in Fig.1. Note that the $NaAlSiO_3$-$KAlSiO_3$-SiO_2 model system constitutes a significant simplification of evolved natural alkali suites, but yet is a very useful conceptualization of what happens with evolved alkali melt compositions.

Most important for melt fractionation of evolved OIB systems is whether the evolving melt approaches the alkali-feldspar thermal divide at lower or higher SiO_2-values, the former case leads melts to evolve to the phonolite-minimum, the latter case to the granite-minimum.

REFERENCES

Assunção, C.F.T., Machado, F., Gomes, R.A.D., 1965, On the occurrence of carbonatites in the Cape Verde Islands. Boletim da Sociedade Geológica de Portugal v. 16, p. 179–188

Balogh, K., Ahijado, A., Casillas, R., Fernàndez, C., 1999, Contributions to the chronology of the Basal Complex of Fuerteventura, Canary Islands. Journal of Volcanological and Geothermal Research v. 90, p. 81-101

Barrera, J.L., Fernandez Santin, S., Fuster, J.M., Ibarrola, E., 1981, Ijolitas-Sienitas-Carbonatitas de los macizos del norte del complejo plutonico basal de Fuerteventura (Islas Canarias). Boletin Geologico Minero, v. 92-94, p. 309-321.

Brooker, R.A., 1998, The effect of CO2 saturation on immiscibility between silicate and carbonate liquids: an experimental study. Journal of Petrology v. 39, p. 1905-1915

Brooker, R.A., Kjarsgaard, B.A., 2011, Silicate-carbonatite liquid immiscibility and phase relations in the system SiO_2-Na_2O-Al_2O_3-CaO-CO_2 at 0.1-2.5 GPa with applications to carbonatite genesis. Journal of Petrology v. 52, p. 1281-1305.

Clague DA, Frey FA (1982) Petrology and trace element geochemistry of the Honolulu Volcanics, Oahu: implications for the oceanic mantle below Hawaii. Journal of Petrology v. 23, p. 447-504.

Fudali, R.F., 1963, Experimental studies bearing on the origin of pseudoleucite and associated problems of alkali rock systems. Geological Society of America Bulletin, v. 74, p. 1101-1126.

Freestone, I.C., Hamilton, D.L., 1980, The role of liquid immiscibility in the genesis of carbonatites – an experimental study. Contributions to Mineralogy and Petrology, v.73, p.105-117.

Frey FA., Clague DA (1983) Geochemistry of diverse basalt types from Loihi Seamount, Hawaii: petrogenetic implications. Earth and Planetary Science Letters v. 66, p. 337-355.

Guzmics T, Mitchell RH, Szabo C, Berkesi M, Milke R, Abart R (2011) Carbonatite melt inclusions in coexisting magnetite, apatite and manticellite in Kerimasi calciocarbonatite, Tanzania: melt evolution and petrogenesis. Contributions of Mineralogy and Petrology v. 161, p. 177-196.

Hamilton, D.L., Freestone, I.C., Dawson, J.B., Donaldson, C.H., 1979, Origin of carbonatites by liquid immiscibility. Nature v. 279, p. 52-54

Holm P.M., Wilson J.R., Christensen B.P., Hansen L., Hansen S.L., Hein K.M., Mortensesn A.K., Pedersen R., Plesner S., Runge M.K., 2006, Sampling the Cape Verde Mantle Plume: Evolution of Melt Compositions on Santo Antão, Cape Verde Islands. Journal of Petrology v. 47, p. 145-189

Hörnle, K., Tilton, G., Le Bas, M.J., Duggen, S., Garbe-Schönberg, D., 2002, Geochemistry of oceanic carbonatites compared with continental carbonatites: mantle recycling of oceanic crustal carbonate. Contributions to Mineralogy and Petrology v. 142, p. 520– 542.

Irvine TN, Baragar WRA (1971) A guide to chemical classification of the common volcanic rocks. Canadian Journal of Earth Sciences v. 8, p. 523-548

Kjarsgaard, B.A., 1998, Phase relations of a carbonated high CaO-nephelinite at 0.2 and 0.5 GPa. Journal of Petrology v. 39, p. 2061-2075.

Kogarko LN, Plant DA, Henderson CMB, Kjarsgaard BA (1991) Na-rich carbonate inclusions in perovskite and calzirtite from the Guli intrusive Ca-carbonatite, polar Sibiria. Contributions to Minerology and Petrology v. 109, p. 124-129.

Luth, W.C., Jahns, R.H., Tuttle, O.F., 1964, The granite system at pressures of 4-10 kilobars. Journal of Geophysical Research, v.69, p. 759-773.

MacDonald GA, Katsura T (1964) Chemical composition of Hawaiian lavas. Journal of Petrology v. 5, p. 82-133.

MacDonald GA, Powers HA (1968) A further contribution to the petrology of Haleakala volcano, Hawaii. Geological Society of America Bulletin v. 79, p. 877-888.

Madeira, J., Mata, J., Mourão, C., Da Silva, A.B., Martins, S., Ramalho, R., Hoffmann, D.L., 2010, Volcano stratigraphic and structural evolution of Brava Island (Cape Verde) based on 40Ar/39Ar, U–Th and field constraints. Journal of Volcanological and Geothermal Research, v. 196, p. 219-235.

Machado F, Azeredo Leme J, Monjardino J, Seita MF (1968) Carta geológica de Cabo Verde, notícia explicativa da Ilha Brava e dos Ilhéus Secos. Garcia de Orta v. 16, p. 123–130

Martin, L.H.J., Schmidt, M.W., Mattsson, H.B., Günther, D., 2013, Element partitioning between immiscible carbonatite and silicate melts for dry and H_2O-bearing systems at 1-3 GPa. Journal of Petrology v. 54, p. 2301-2338.

Mourão C, Mata J, Doucelance R, Madeira J, da Silva AB, Silva LC, Moreira M (2010) Quaternary extrusive calciocarbonatite volcanism on Brava Island (Cape Verde): A nephelinite-carbonatite immiscibility product. Journal of African Earth Sciences v. 56, p. 59-74

Naughton JJ, MacDonald GA, Greenberg, VA (1980) Some additional potassium-argon ages of Hawaiian rocks: the Maui volcanic complex of Molokai, Maui, Lanai and Kahoolawe. Journal of Volcanological and Geothermal Research v. 7, p. 339-355.

Nielsen TFD, Solovova IP, Veksler IV (1997) Parental melts of melilotite and origin of alkaline carbonatite: evidence from crystallized melt inclusions, Gardiner complex. Contributions to Mineralogy and Petrology v. 126, p. 331-344.

Panina LI (2005) Multiphase carbonate-salt immiscibility in carbonatite melts: data on melt inclusions from the Krestovskiy massif minerals (Polar Siberia). Contributions to Mineralogy and Petrology v. 150, 19-36.

Panina, L.I., Motorina, I.V., 2008, Liquid immiscibility in deep-seated magmas and the generation of carbonatite melts. Geochemistry International v. 46, p. 448-464.

Schairer, J.F., 1957, Melting relations of the common rock forming oxides. Journal of the American Ceramic Society, v.40, p.215-135.

Sisson TW, Kimura JI, Coombs ML (2009) Basanite-nephelinite suite from early Kilauea: carbonated melts of phlogopite-garnet peridotite at Hawaii's leading magmatic edge. Contributions to Mineralogy and Petrology v. 158, 803-829.

Taylor, D., MacKenzie, W.S., 1975, A contribution to the pseudoleucite problem. Contributions to Mineralogy and Petrology, v. 49, p. 321-333.

Tuttle, O.F., Bowen, N.L., 1958, Origin of granite in the light of experimental studies in the system $NaAlSi_3O_8$-$KAlSi_3O_8$-SiO_2. Geological Society of America Memoir 74, 153 p.

Zeng, R.S., MacKenzie, W.S., 1984, Preliminary report on the system $NaAlSiO_4$-$KAlSiO_4$-SiO_2 at $P(H_2O)$ = 5 kbar. Bulletin Mineralogique, v. 107, p. 571-577.

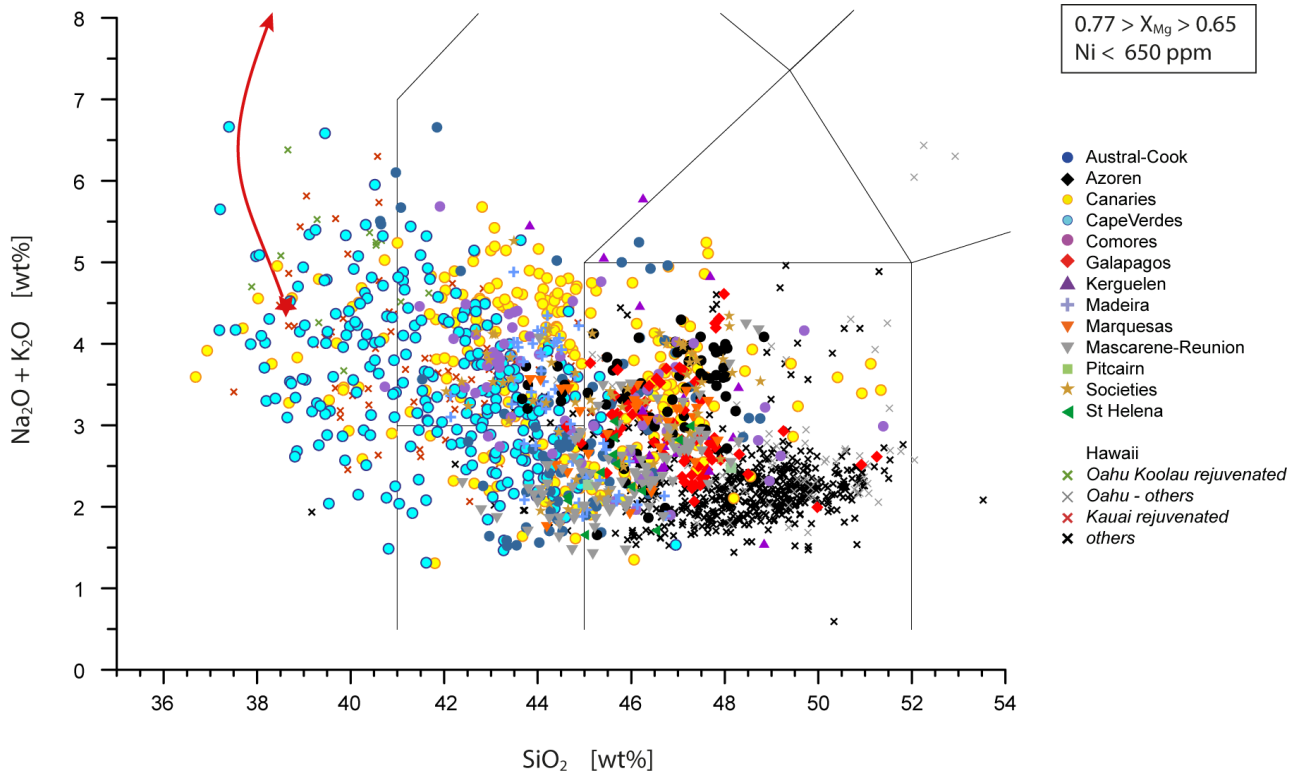

Figure DR1: Primitive melts with boundary lines of the TAS diagram, the red star and arrow indicate the primitive melt and the fractionation path that led to carbonate – silicate liquid immiscibility on Brava (Weidendorfer et al., 2016).

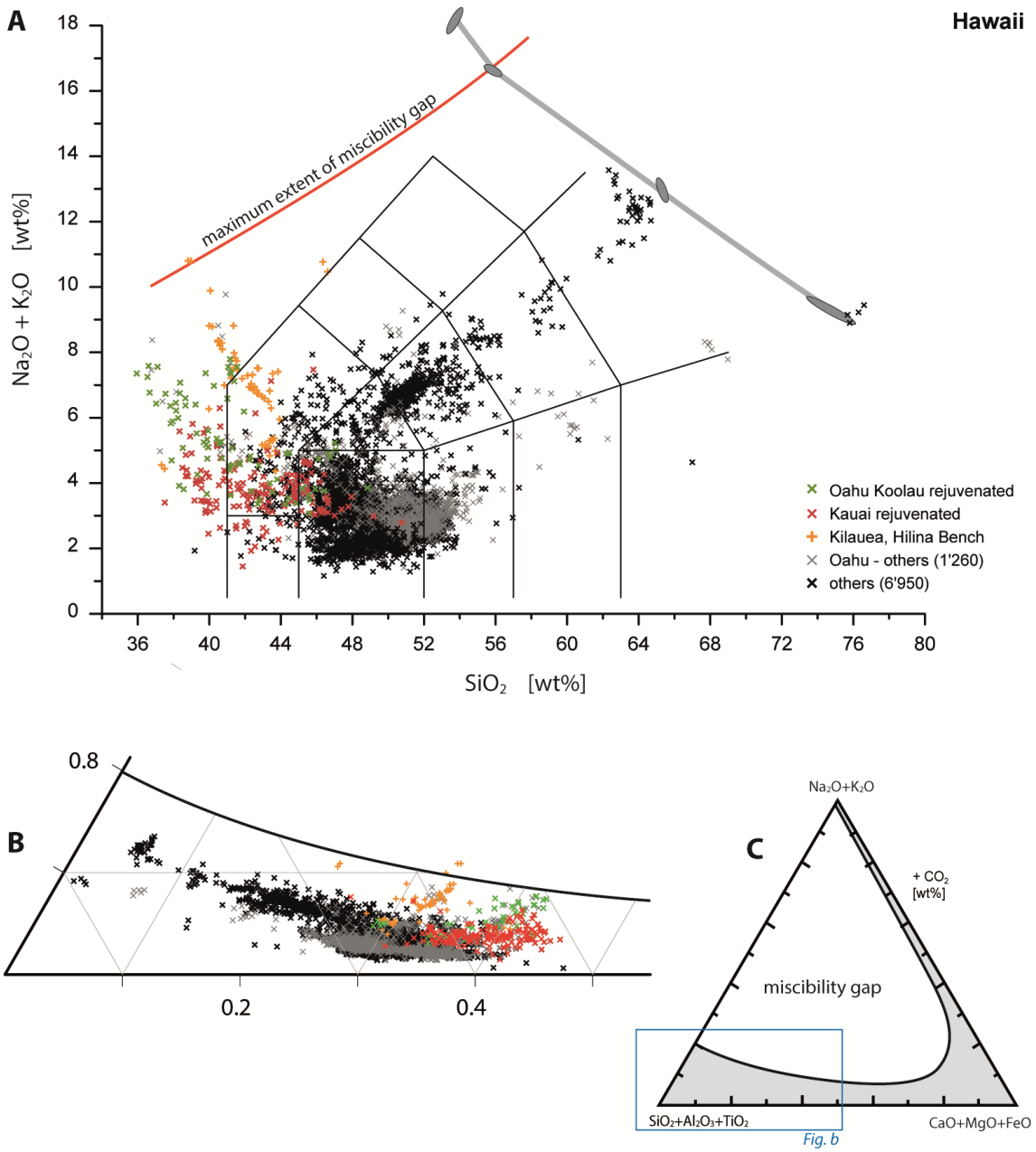

Figure DR2: Hawaii: (a) TAS diagram, the largest part of the 9'000 analyses follows a tholeiitic trend, nevertheless, a smaller part has a sub-alkaline trend evolving towards the alkali feldspar thermal divide. (b) Si-rich corner of the Na_2O+K_2O – $SiO_2+TiO_2+Al_2O_3$ – CaO+FeO+MgO ternary for Hawaii. Three units have a low-Si, high-alkali chemistry, namely Hilina bench on Kilauea, and the rejuvenated stages of Kauai and Oahu. (c) Schematic Na_2O+K_2O – $SiO_2+TiO_2+Al_2O_3$ – CaO+FeO+MgO ternary including the maximum extend of melt miscibility gap based on Kjarsgaard (1998), Brooker (1998), Brooker and Kjarsgaard (2011), and Martin et al. (2013).

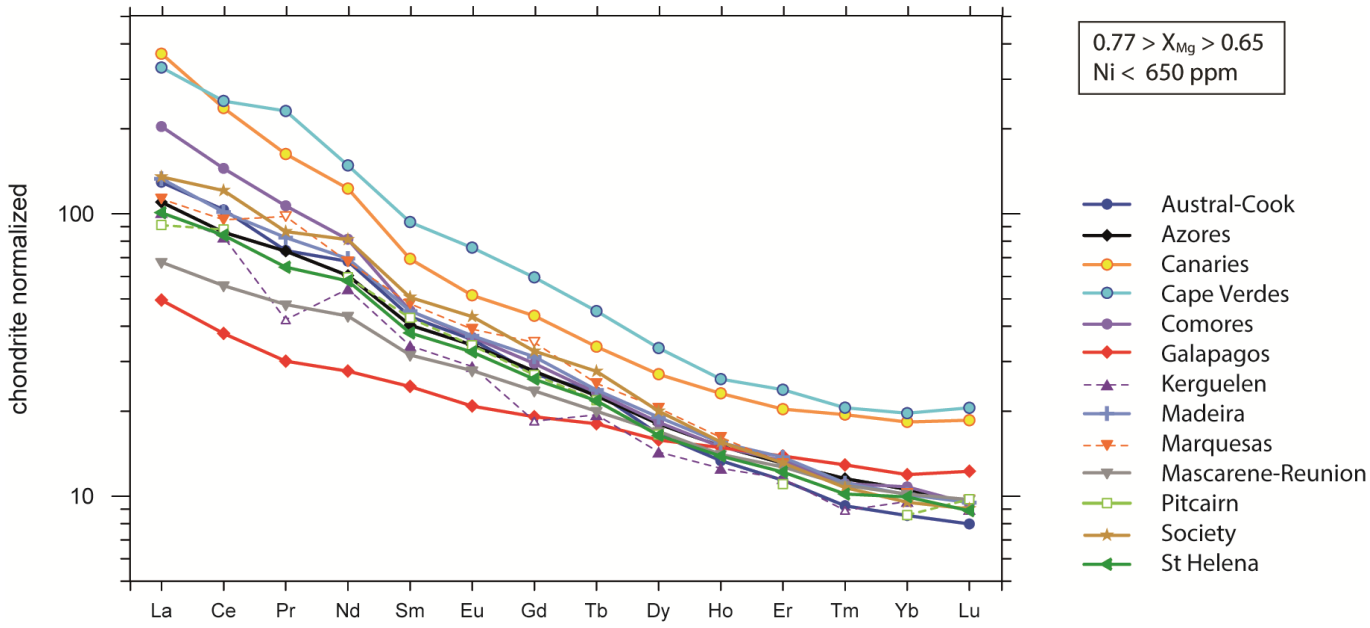

Figure DR3: Chondrite normalized average REE patterns of primitive melts (X_{Mg}=0.77-0.65) from the 15 hot spots with primitive melts. Note that the Canaries and Cape Verdes have the highest REE likely indicating lower degrees of melting. The Galapagos melts are closest to E-MORB, not a surprise as the Galapagos hot spot interferes with the East Pacific Rise.

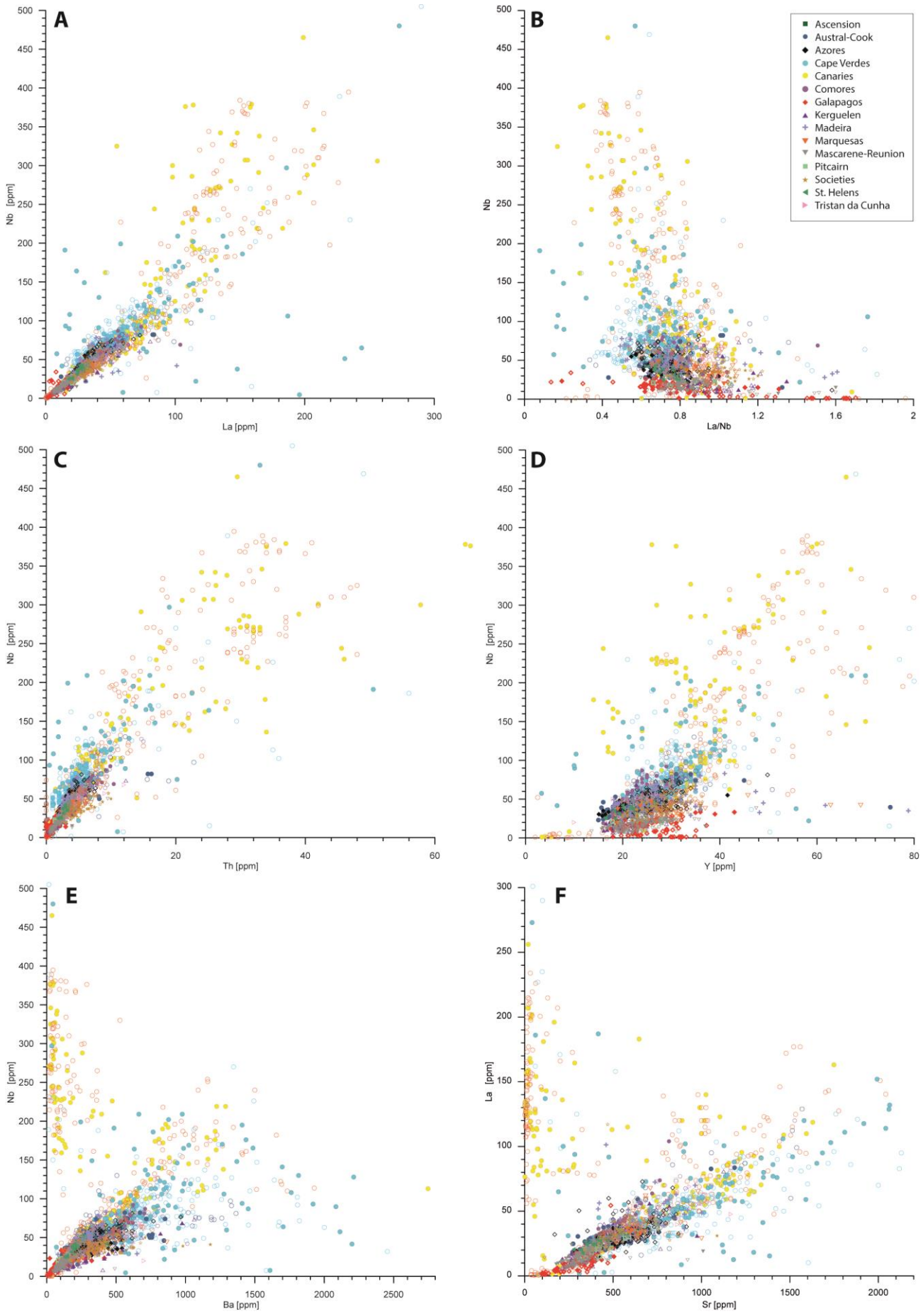
A
Nb [ppm]
La [ppm]
B
Nb
La/Nb
Ascension
Austral-Cook
Azores
Cape Verdes
Canaries
Comores
Galapagos
Kerguelen
Madeira
Marquesas
Mascarene-Reunion
Pitcairn
Societies
St. Helens
Tristan da Cunha
C
Nb [ppm]
Th [ppm]
D
Nb [ppm]
Y [ppm]
E
Nb [ppm]
Ba [ppm]
F
La [ppm]
Sr [ppm]

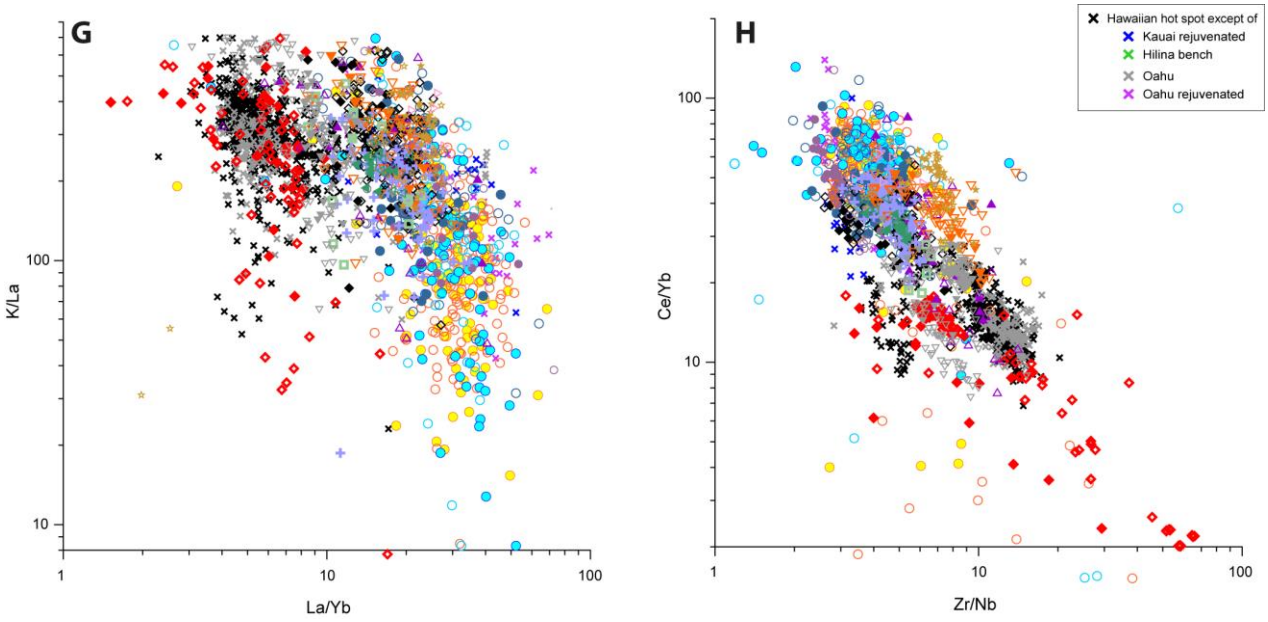

Figure DR4 (A-G): K-Nb-Zr-Y-Sr-Ba-La-LREE/HREE systematics (for Nb-Zr-Rb-Sr see text) for samples with X_{Mg}=0.77-0.55. Closed symbols X_{Mg}=0.77-0.65, open symbols X_{Mg}=0.65=0.55. For most of the Cape Verdes and Canaries and for all other hot spots investigated here, incompatible trace elements correlate positively. Within this array, only the Cape Verdes and Canaries have abundant analyses at >80 ppm Nb, >400 ppm Zr, >60 ppm La, >600 ppm Ba, >900 ppm Sr and > 50 ppm Rb, which are likely the result of smaller degrees of melting for eruption products that have reached the surface.

The trace systematics changes above 120 ppm Nb (see also Fig. 3): The Cape Verdes and Canaries have a high Nb-Zr-REE-Rb but low Sr-Ba component which does not correlate with major element chemistry or any rock unit but occurs occasionally in all units (including the carbonatite bearing ones). This component is interpreted as metasomatic phlogopite±Ti-oxide in the lithosphere, precipitated from an earlier plume melt which had Sr and Ba removed by a lower temperature carbonate-rich melt or fluid that migrated further. Both components are apparently assimilated on occasion. LREE/HREE most likely translate to the amount of garnet in the source, i.e. to the source pressure.

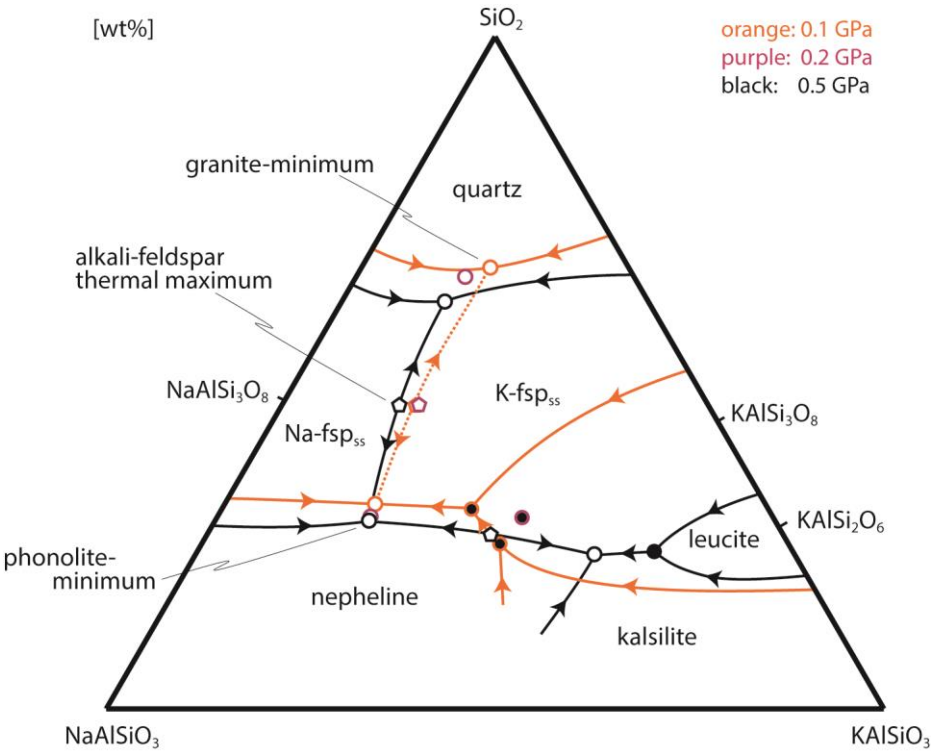

Figure DR5: $NaAlSiO_3$-$KAlSiO_3$-SiO_2 system at 0.1-0.5 GPa H_2O-pressure. Open circles are minima or eutectic points, filled circles peritectic points, pentagons are thermal divides or maxima. The stippled line traces the minimum on the feldspar-liquidus surface and is not a cotectic line. Note that the alkali-feldspar thermal divide is a local maximum on this line (or on the 0.5 GPa cotectic) yet still a minimum on the feldspar join.